17. R. Yasuda et al., Nat. Neurosci. 9, 283 (2006).
18. N. Mochizuki et al., Nature 411, 1065 (2001).
19. O. Rocks et al., Science 307, 1746 (2005).
20. D. W. Piston, D. R. Sandison, W. W. Webb, in Time-Resolved Laser Spectroscopy in Biochemistry III, J. R. Lakowicz, Ed. (SPIE, Bellingham, WA, 1992), pp. 379–389.
21. E. Gratton, S. Breusegem, J. Sutin, Q. Ruan, N. Barry, J. Biomed. Opt. 8, 381 (2003).
22. Supporting online material is available on Science Online.
23. E. A. Nimchinsky, R. Yasuda, T. G. Oertner, K. Svoboda, J. Neurosci. 24, 2054 (2004).
24. C. D. Kopec, B. Li, W. Wei, J. Boehm, R. Malinow, J. Neurosci. 26, 2000 (2006).
25. M. Fivaz, S. Bandara, T. Inoue, T. Meyer, Curr. Biol. 18, 44 (2008).
26. G. H. Patterson, J. Lippincott-Schwartz, Science 297, 1873 (2002).
27. E. A. Reits, J. J. Neefjes, Nat. Cell Biol. 3, E145 (2001).
28. H. Niv, O. Gutman, Y. Kloog, Y. I. Henis, J. Cell Biol. 157, 865 (2002).
29. P. H. Lommerse et al., Biophys. J. 86, 609 (2004).
30. A. Losonczy, J. K. Makara, J. C. Magee, Nature 452, 436 (2008).
31. We thank N. Ghitani, B. Burbach, C. Zhang, B. Shields, and H. White for technical assistance; N. Gray for help with immunostaining; L. van Aelst for helpful discussions; and J. Dudman for comments on the manuscript. This work was supported by the Howard Hughes Medical Institute, NIH, a David and Fanny Luke Fellowship (C.D.H.), Burroughs Wellcome Fund (R.Y.), Dana Foundation (R.Y.), National Alliance for Autism Research (R.Y.), National Institute of Mental Health (R.Y.), and National Alliance for Research on Schizophrenia and Depression (H.Z.).

Finite Scale of Spatial Representation in the Hippocampus

Kirsten Brun Kjelstrup,[1] Trygve Solstad,[1] Vegard Heimly Brun,[1] Torkel Hafting,[1] Stefan Leutgeb,[1] Menno P. Witter,[1,2] Edvard I. Moser,[1]* May-Britt Moser[1]

To determine how spatial scale is represented in the pyramidal cell population of the hippocampus, we recorded neural activity at multiple longitudinal levels of this brain area while rats ran back and forth on an 18-meter-long linear track. CA3 cells had well-defined place fields at all levels. The scale of representation increased almost linearly from <1 meter at the dorsal pole to ~10 meters at the ventral pole. The results suggest that the place-cell map includes the entire hippocampus and that environments are represented in the hippocampus at a topographically graded but finite continuum of scales.

Although the basic intrinsic circuitry of the hippocampus is similar along the entire dorsoventral axis of the structure (1), dorsal and ventral regions may not have similar functions. Dorsal and intermediate regions are preferentially connected, via the dorsolateral and intermediate bands of the entorhinal cortex, to visual and somatosensory cortices important for accurate spatial navigation (2–5), and selective lesions in these hippocampal regions can lead to impairments in spatial learning (6–8). Pyramidal cells in these parts of the hippocampus have spatially selective firing fields that reflect the animal's location (9, 10) and jointly form a maplike representation of the environment (10–12). The scale of this representation increases from dorsal to intermediate hippocampus (13, 14), matching the progressive dorsoventral increase in the spacing of grid cells in medial entorhinal cortex, one synapse upstream (15, 16). In contrast, the ventral one-third of the hippocampus has strong connections with a restricted number of interconnected areas of the lateral septum, hypothalamus, and amygdala, both directly and through the ventromedial portions of the entorhinal cortex (2, 17–19). Selective lesions of the ventral hippocampus affect autonomic and defensive responses but not basic spatial behaviors (20, 21). Collectively, these studies imply a functional division in the hippocampus where the dorsal and intermediate parts are more important for spatial behavior and the ventral part is more relevant for emotional and motivational processes. However, such a division does not rule out the possibility that location is represented at all levels of the hippocampus. Spatial inputs may reach even the most ventral cells via the associational networks of the hippocampus (22, 23) or by way of intrinsic connections between dorsal and ventral parts of the entorhinal cortex (3). To determine whether the ventral hippocampus also has place cells, we compared neural activity at multiple longitudinal levels of CA3 in 21 rats (24). All recording sites were mapped onto the long axis of CA3 (fig. S1). The data were subdivided into three groups based on recording location (dorsal, 7 to 22%; intermediate, 40 to 70%; and ventral, 70 to 100%).

Conventional recording environments may be too small to visualize the most extended hippocampal representations (figs. S2 to S4 and supporting online text). Thus, we tested the animals on an 18-m-long linear track. Well-delineated place fields, defined as spatially stable contiguous regions with firing above 20% of the peak rate, could be found at all longitudinal levels of the hippocampus (Fig. 1 and fig. S5). The representations scaled up between dorsal and ventral recording locations (Fig. 1), from an average place field size of 0.98 ± 0.03 m in dorsal hippocampus (mean $\pm$ SEM; 111 cells, five rats), to 3.73 ± 0.43 m in intermediate hippocampus (37 cells, three rats), and 5.52 ± 0.54 m in ventral hippocampus (61 cells, four rats). Few fields were longer than 10 m. The relation between recording location and field size was strong (dorsal versus intermediate versus ventral: $F_{2,517} = 86.5$, $P < 0.001$; all pairwise comparisons significant at $P < 0.001$, Bonferroni test). Forty-five per cent of the variance was explained by a linear regression model [$r = 0.67$, $n = 111$, $P < 0.001$; (fig. S6)]. There was a similar increase in the width of the central peak of the spatial autocorrelation function, measured at 20% of the peak value (dorsal, 1.12 ± 0.03 m; intermediate, 3.07 ± 0.19 m; and ventral, 4.10 ± 0.18 m; $F_{2,327} = 179.8$, $P < 0.001$; all pairwise comparisons significant at $P < 0.001$). In this case, 53% of the variance was explained by a linear regression model [$r = 0.73$, 111, $P < 0.001$; (fig. S6; supporting online text)].

The size of individual hippocampal place fields can also be estimated by exploiting the fact that place cells exhibit theta phase precession (25). A place field can be defined as the area between the points on a track where the precession begins and terminates (26). Running on the 18-m track was associated with theta rhythmicity and phase precession at all dorsoventral recording levels in CA3 (81 place cells; Fig. 2 and fig. S7). As the rat crossed the firing field, the firing phase advanced gradually, up to 360°, over successive cycles of the theta rhythm. The strength of precession was estimated for each firing field by rotating the phase by position distribution in steps of 1° across the phase cycle and fitting a linear regression line for each rotation (25, 27). The rotation that gave the largest explained variance was identified. The slope of the regression line at this rotation (phase change per unit of movement) decreased as the field size increased along the long axis of the hippocampus (Fig. 2). In the ventral CA3, the phase advance often occurred over distances as large as 10 m (Fig. 2, right). The mean regression slope changed from $-102° \pm 33°$ per meter in dorsal hippocampus ($t_{62} = 3.1$, $P < 0.005$) to $-18° \pm 9°$ per meter in intermediate and ventral hippocampus ($t_{37} = 2.09$, $P < 0.05$; group difference: $t_{99} = 2.3$, $P < 0.05$; intermediate and ventral cells were combined be-

[1]Kavli Institute for Systems Neuroscience and Centre for the Biology of Memory, Norwegian University of Science and Technology, 7489 Trondheim, Norway. [2]Research Institute Neurosciences, Department of Anatomy and Neurosciences, VU University Medical Center, 1007 MB Amsterdam, Netherlands.

*To whom correspondence should be addressed. E-mail: edvard.moser@ntnu.no

cause of low numbers). The 5- to 10-fold increase in the distance covered by one cycle of precession is consistent with the 5- to 10-fold increase in the width of the place fields. Precession over such long distances also implies that the active firing regions in the ventral hippocampus are part of one place field rather than multiple overlapping fields.

The somewhat irregular shape of the ventral hippocampal place fields makes it difficult to estimate field size accurately because the algorithm sometimes cleaves fields as a result of local rate variations (see examples in Fig. 1 and fig. S5) and because fields at the end of the track may be truncated. To reduce the impact of these varia-bles, we combined data from multiple recordings in a population vector analysis (Fig. 3 and fig. S8). Rate maps were stacked separately for left and right running directions, and the length of the track was segmented into 5-cm bins, giving a total of 330 population vectors per running di-rection after exclusion of the turning points. The correlation between all pairs of population vec-tors was plotted in a color-coded matrix where the correlation of each population vector with itself is represented along the diagonal (14, 28). The width of the band of high correlations along the diagonal provides an indication of the size of a typical place field, without the constraints caused by cell-specific rate and shape variations. The mean half-width (at $r = 0.50$) was 0.81 m for dorsal CA3, 3.71 m for intermediate CA3, and 6.66 m for ventral CA3 (Fig. 3). The mean width at $r = 0.20$ was 1.41 m (dorsal), 8.65 m (intermediate), and 13.59 m (ventral). As was true for the analyses for individual cells, the relation between position on the dorsoventral axis and width of the correlated band was approxi-mately linear (Fig. 4).

This study has two main findings. First, place cells exist along the entire longitudinal axis of the hippocampus, even in the most ventral region where the connectivity with somatosensory and

Fig. 1. Place fields of eight pyramidal cells rec-orded at different longi-tudinal levels of CA3 during animals' running on a linear 18-m track. (**A**) Nissl-stained sections showing recording loca-tions in four animals. Individual rat numbers are indicated. (**B**) Place fields on the 18-m track. Each panel shows one cell. Rat numbers refer to (A). Percentages indi-cate location along the dorsoventral axis. For rat 11285, only the 87% lo-cation is shown in (A). (Top of each panel) Smoothed spike density function indicates firing rate as a function of position. Horizontal bar indicates estimated place field. Left runs, red; right runs, green. (Bottom of each panel) Raster plot showing density of spikes on individual laps. Each vertical tic indicates one spike and each hor-izontal line shows one lap (right side, blue-green; left, red). See fig. S5 for complete cell samples. Note 5- to 10-m-long place fields in ventral CA3 (colored hor-izontal bars; left runs, red; right runs, green).
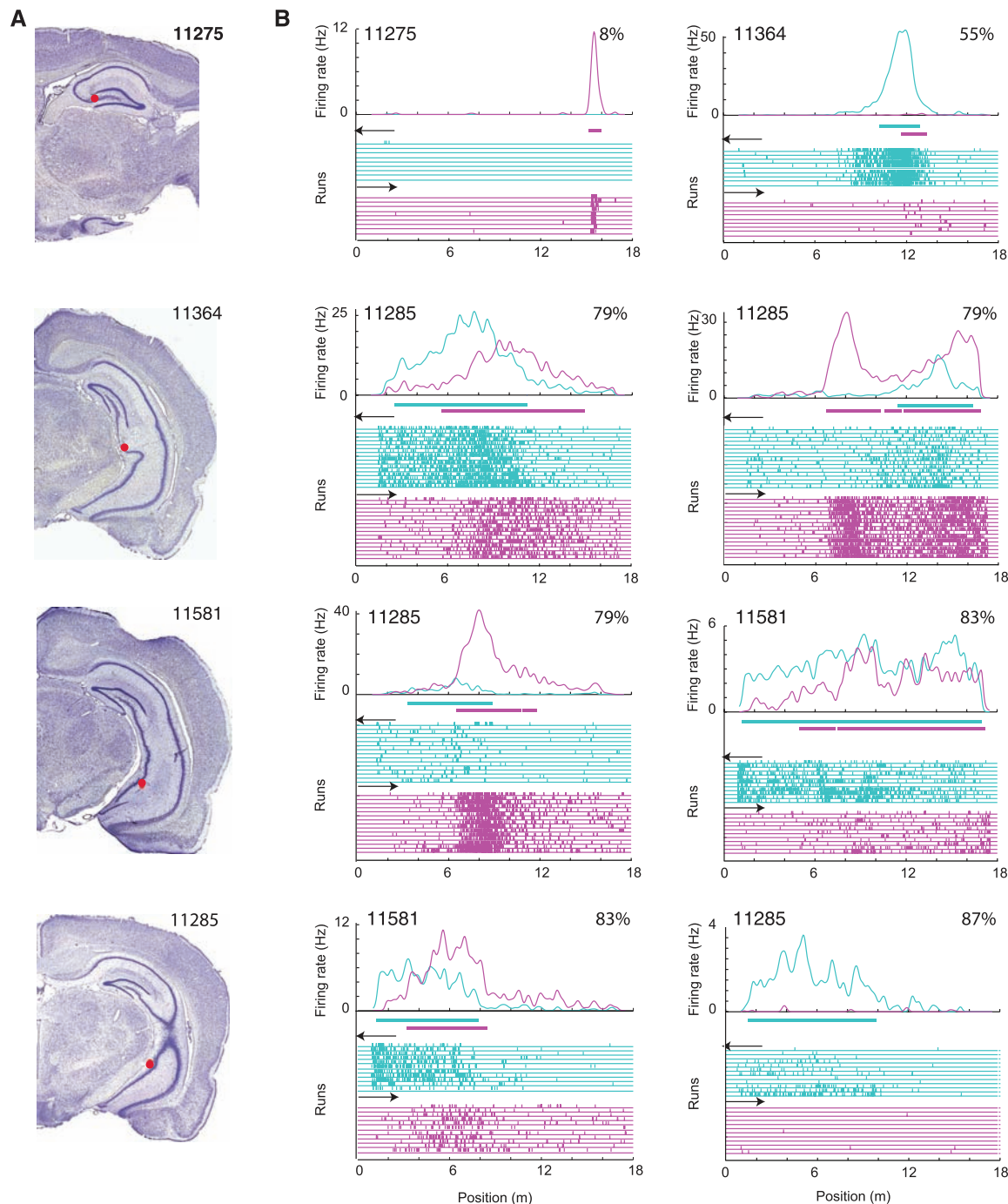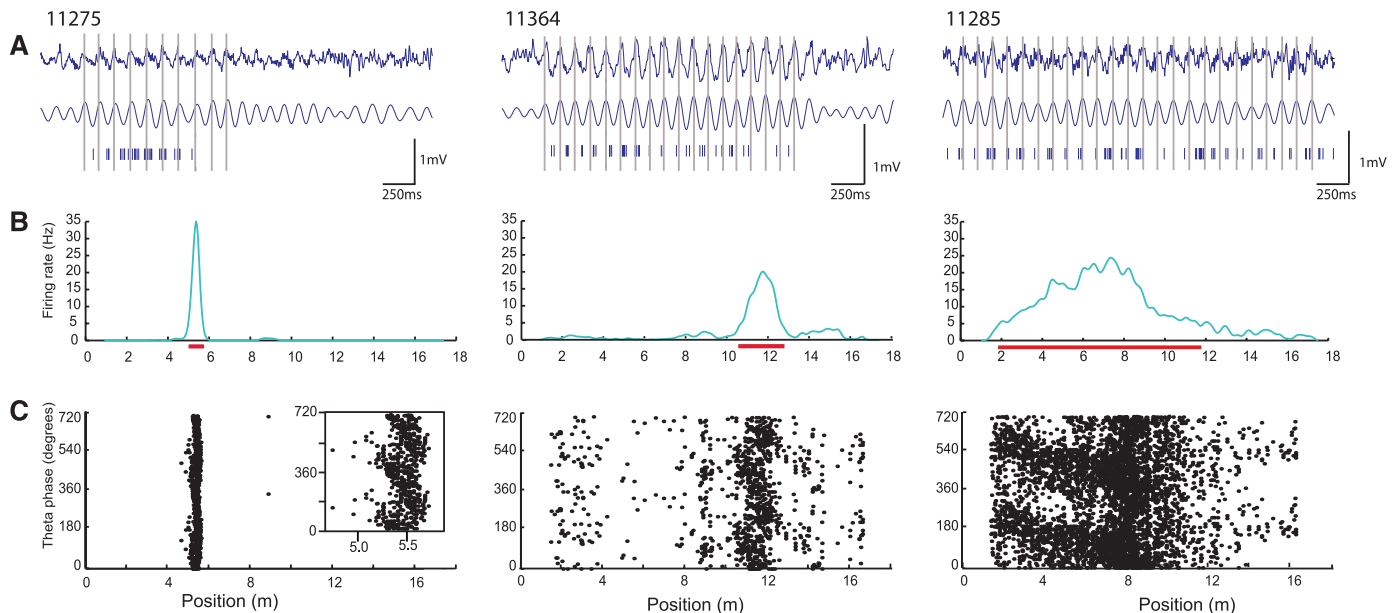
Fig. 2. Reduced rate of theta-phase precession in ventral hippocampus. Three cells are shown (left) dorsal CA3, (middle) intermediate CA3, and (right) ventral CA3. Rats and recording positions are the same as in Fig. 1. Only right runs are shown. (**A**) Local EEG with spike times (3.0 s). (Top trace) unfiltered; (bottom trace) 5 to 11 Hz filtered. Gray vertical lines indicate peak of theta cycle (0° or 360°). Individual spikes are shown as small vertical tics. (**B**) Smoothed spike density function showing size and location of firing field on the 18-m track. Red horizontal bar indicates estimated extent of place field. (**C**) Theta phase (two cycles) as a function of position. Each dot corresponds to one spike. For the dorsal cell, the phase-position field is magnified in the inset. Note 5- to 10-fold increase in the distance covered by one cycle of precession as field size increases toward the ventral hippocampus.

Fig. 3. Population vector autocorrelograms showing graded increase in spatial scale (**A**) dorsal, (**B**) intermediate, and (**C**) ventral CA3. (Left and middle) Linear rate maps of all pyramidal cells from each location were stacked, and a population vector was defined for each 5-cm bin of the composite map. Pearson's product moment correlation coefficient was calculated for each pair of population vectors, giving a two-dimensional correlation matrix. Correlation is color-coded (for r between −1 and 0, color is blue; color scale from 0 to 1 is linear, as shown on the scale bar). The width of the diagonal color band indicates the distance over which successive population vectors become decorrelated (*14*, *28*). Arrows indicate running direction; see fig. S8 for both directions. (Line graphs) Correlation as a function of spatial distance between population vectors. Horizontal lines indicate half-width (*14*) and 20% width.
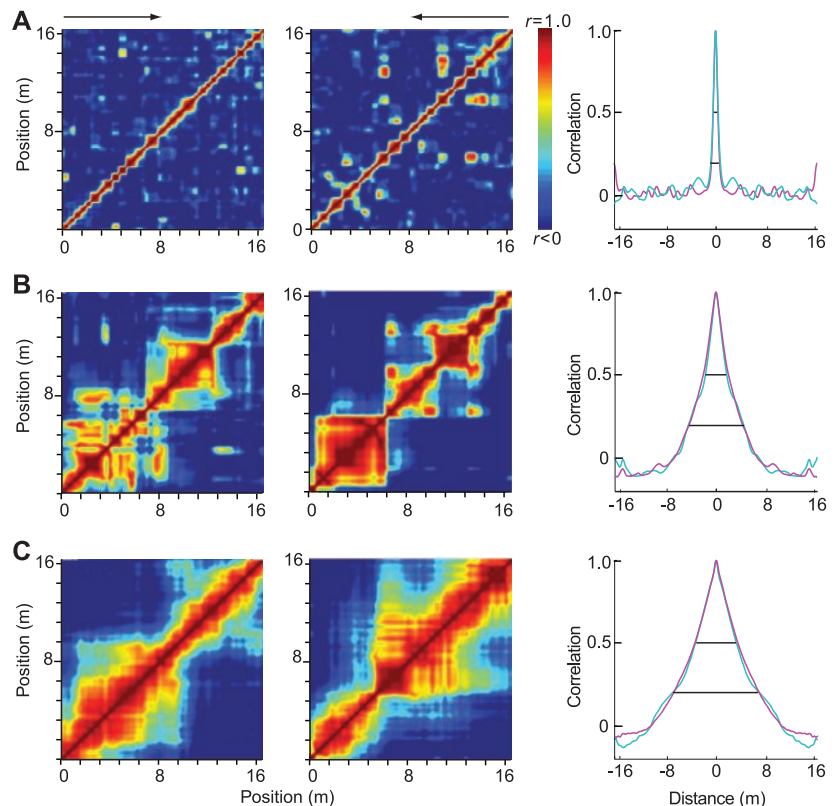

visual brain regions is less direct (*2–5*, *29*). The origin of the spatial inputs to the ventral hippocampus is not known, but spatial information can probably reach ventral parts of the hippocampus both by way of associational fibers from place cells in the dorsal hippocampus (*22*) and by way of projections from grid cells in the intermediate-to-ventral medial entorhinal cortex, if these exist (*30*). The presence of place cells in the ventral hippocampus suggests that parts of hypothalamus and amygdala involved in motivation and emotion receive significant information about the general location or spatial context of the animal.

The second main finding is that the scale of the hippocampal representation is topographical-

Fig. 4. Spatial scale as a function of position along the dorsoventral (DV) axis of the hippocampus. Scale is expressed as the half-width of the correlated band in the population vector analyses (Fig. 3), as the average width of the largest place field of individual cells (mean ± SEM), or as the estimated field width based on the slope of the best-fit linear regression line for the position versus phase distribution. The population estimate is more likely to reflect the true spatial scale because the algorithm for detecting individual place fields occasionally divided fields as a consequence of local rate variations.
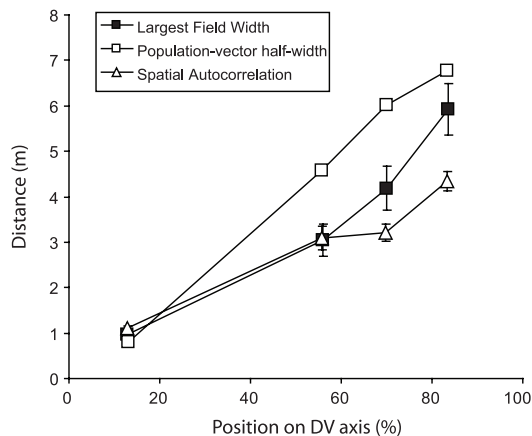
ly graded, much like representations in some sensory maps of the brain (*31, 32*). The spatial map expands approximately linearly from a scale of <1 m near the dorsal pole to ~10 m near the ventral pole (*33*). Within this range, the hippocampus can represent environments at multiple spatial scales and levels of detail, up to a given limit. The upper limit of ~10 m may be sufficiently large to enable the hippocampus to form detailed representations of all environments within the rat's home range, which has an average radius of about 30 to 50 m (*34, 35*). A challenge for future research will be to determine whether place cells scale up further in mammals with larger territorial radii.

References and Notes

1. P. Andersen, T. V. P. Bliss, K. K. Skrede, *Exp. Brain Res.* **13**, 222 (1971).
2. M. P. Witter, H. J. Groenewegen, F. H. Lopes da Silva, A. H. M. Lohman, *Prog. Neurobiol.* **33**, 161 (1989).
3. C. L. Dolorfo, D. G. Amaral, *J. Comp. Neurol.* **398**, 49 (1998).
4. K. M. Kerr, K. L. Agster, S. C. Furtak, R. D. Burwell, *Hippocampus* **17**, 697 (2007).
5. S. C. Furtak, S. M. Wei, K. L. Agster, R. D. Burwell, *Hippocampus* **17**, 709 (2007).
6. E. Moser, M.-B. Moser, P. Andersen, *J. Neurosci.* **13**, 3916 (1993).
7. M.-B. Moser, E. I. Moser, *J. Neurosci.* **18**, 7535 (1998).
8. M.-B. Moser, E. I. Moser, *Hippocampus* **8**, 608 (1998).
9. J. O'Keefe, J. Dostrovsky, *Brain Res.* **34**, 171 (1971).
10. E. I. Moser, E. Kropff, M.-B. Moser. *Annu. Rev. Neurosci.* **31**, in press.
11. J. O'Keefe, L. Nadel, *The Hippocampus as a Cognitive Map* (Clarendon, Oxford, 1978).
12. M. A. Wilson, B. L. McNaughton, *Science* **261**, 1055 (1993).
13. M. W. Jung, S. I. Wiener, B. L. McNaughton, *J. Neurosci.* **14**, 7347 (1994).
14. A. P. Maurer, S. R. VanRhoads, G. R. Sutherland, P. Lipa, B. L. McNaughton, *Hippocampus* **15**, 841 (2005).
15. M. Fyhn, S. Molden, M. P. Witter, E. I. Moser, M.-B. Moser, *Science* **305**, 1258 (2004).
16. T. Hafting, M. Fyhn, S. Molden, M.-B. Moser, E. I. Moser, *Nature* **436**, 801 (2005).
17. P. Y. Risold, L. W. Swanson, *Science* **272**, 1484 (1996).
18. M. Pikkarainen, S. Rönkkö, V. Savander, R. Insausti, A. Pitkänen, *J. Comp. Neurol.* **403**, 229 (1999).
19. G. D. Petrovich, N. S. Canteras, L. W. Swanson, *Brain Res. Brain Res. Rev.* **38**, 247 (2001).
20. D. M. Bannerman *et al.*, *Behav. Neurosci.* **116**, 884 (2002).
21. K. G. Kjelstrup *et al.*, *Proc. Natl. Acad. Sci. U.S.A.* **99**, 10825 (2002).
22. D. G. Amaral, M. P. Witter, *Neuroscience* **31**, 571 (1989).
23. H. A. Steffenach, R. S. Sloviter, E. I. Moser, M.-B. Moser, *Proc. Natl. Acad. Sci. U.S.A.* **99**, 3194 (2002).
24. Materials and methods are available as supporting material on *Science* Online.
25. J. O'Keefe, M. L. Recce, *Hippocampus* **3**, 317 (1993).
26. A. P. Maurer, S. L. Cowen, S. N. Burke, C. A. Barnes, B. L. McNaughton, *Hippocampus* **16**, 785 (2006).
27. M. R. Mehta, A. K. Lee, M. A. Wilson, *Nature* **417**, 741 (2002).
28. K. M. Gothard, W. E. Skaggs, B. L. McNaughton, *J. Neurosci.* **16**, 8027 (1996).
29. Previous studies have demonstrated place fields in intermediate parts of the hippocampus, at approximately 30 to 45% of the dorsal-to-ventral axis (*13, 14*). Ventral place cells were also reported in another study (*36*) but because this study did not include histological assessment of the recording locations and because the size of the fields was similar to that of dorsal place cells, it is hard to compare the results.
30. T. Solstad, V. H. Brun, K. B. Kjelstrup, M. Fyhn, M. P. Witter, E. I. Moser, M.-B. Moser. *Soc. Neurosci. Abstr.* **33**, 93.2 (2007).
31. T. McLaughlin, D. D. M. O'Leary, *Annu. Rev. Neurosci.* **28**, 327 (2005).
32. J. G. Flanagan, *Curr. Opin. Neurobiol* **16**, 59 (2006).
33. Place fields on left and right runs on the 18-m track were more correlated in ventral CA3 than in dorsal CA3, where representations for different directions are often maximally orthogonalized (*37*) (see supporting online text). This suggests that when a large environment is experienced as connected, as on the track, a single extended representation may be formed in the ventral hippocampus. For discrete environments, ventral CA3 still had strongly orthogonalized place maps (supporting online text).
34. W. B. Jackson, in *Wild Mammals of North America*, J. A. Chapman and G. A. Feldhamer, Eds. (Johns Hopkins Univ. Press, Baltimore, MD, 1982), pp. 1077–1088.
35. D. C. Stroud, *J. Mammal.* **63**, 151 (1982).
36. B. Poucet, C. Thinus-Blanc, R. U. Muller, *Neuroreport* **5**, 2045 (1994).
37. S. Leutgeb, J. K. Leutgeb, A. Treves, M.-B. Moser, E. I. Moser, *Science* **305**, 1295 (2004).
38. We thank R. Skjerpeng for programming; L. Colgin, M. Fyhn, and F. Tuvnes for assistance with experiments or analyses; and A. M. Amundsgård, I. M. F. Hammer, K. Haugen, K. Jenssen, B. H. Solem, and H. Waade for technical assistance. The work was supported by the Centre of Excellence scheme of the Norwegian Research Council and the Kavli Foundation.

Finite Scale of Spatial Representation in the Hippocampus
Kirsten Brun Kjelstrup, Trygve Solstad, Vegard Heimly Brun,
Torkel Hafting, Stefan Leutgeb, Menno P. Witter, Edvard I. Moser
and May-Britt Moser (July 4, 2008)
Science **321** (5885), 140-143. [doi: 10.1126/science.1157086]

Editor's Summary

Article Tools	Visit the online version of this article to access the personalization and article tools: http://science.sciencemag.org/content/321/5885/140
Permissions	Obtain information about reproducing this article: http://www.sciencemag.org/about/permissions.dtl